Adaptive High Temperature Superconducting Filters for Interference Rejection

Kurt F. Raihn, Neal O. Fenzi, *Member, IEEE,* Gregory L. Hey-Shipton, *Member, IEEE,* Elna R. Saito, P. Vince Loung, and David L. Aidnik

Abstract— **An optically switched high temperature superconducting (HTS) band-reject filter bank is presented. Fast low loss switching of high quality (Q) factor HTS filter elements enables digital selection of arbitrary pass-bands and stop-bands. Patterned pieces of GaAs and silicon are used in the manufacture of the photosensitive switches. Fiber optic cabling is used to transfer the optical energy from an LED to the switch. The fiber optic cable minimizes the thermal loading of the filter package and de-couples the switch's power source from the RF circuit. This paper will discuss the development of a computer-controlled HTS bank of optically switchable, narrow band, high Q bandstop filters which incorporates a cryocooler to maintain the 77 K operating temperature of the HTS microwave circuit.**

I. Introduction

THE development of switchable and highly selective bandstop filters with low insertion loss will minimize receiver interference problems in dense signal environments. YIG filters have been used in this capacity. The main limitations of YIG filters for use in front end filtering is their insertion loss and tuning speed. Cascading even a few YIG filters will degrade the noise figure of a receiver considerably. YIG filters tune from one frequency to another in several milliseconds, when microseconds is desired. Circuits manufactured using thin-film high temperature superconductors (HTS) exhibit lower conductor losses than do conventional materials. Thin-film HTS circuits are small in size and weight and also offer high quality (Q) factors necessary for constructing very selective filters. Due to the planar topology of the thin-film HTS, solid state photosensitive switches can be used to give switching times faster than possible with YIG filters. Adaptive filters can also be used in cellular receiver base stations where interference is a problem. The sharper skirts of the HTS filters will minimize the signals lost due to crossover interference and also give increased bandwidth which translates into more phone calls being received at one time. A cellular HTS filter will also be much smaller than conventional filters making it feasible to construct more cell sites. By increasing the number of cell sites, the number of calls that can be received increases.

This paper focuses on the development of a computer-controlled, cryocooled HTS bank of optically switchable, narrow band, bandstop filters. The contiguous channels of the filter bank are capable of being configured in many possible combinations to pass desired bands and surgically excise unwanted signals.

Manuscript received October 16, 1995; revised February 12, 1996. This work was supported by ARPA, WPAFB Aeronautical Systems Center, and WPAFB Wright Laboratory.

The authors are with Superconductor Technologies Inc., Santa Barbara, CA 93111-2310 USA.

Publisher Item Identifier S 0018-9480(96)04785-0.

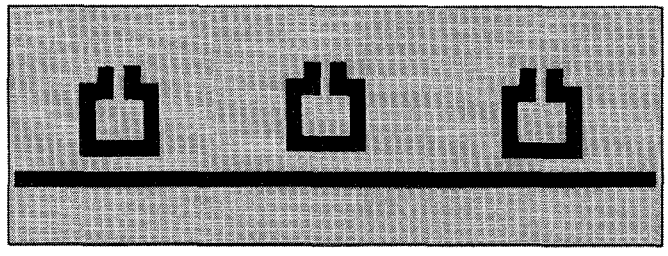

Fig. 1. Three-resonator bandstop filter layout.

II. Bandstop Filters

A. Design

Fig. 1 shows the layout of a typical three-resonator bandstop filter. Note that the resonators are rectangular in shape and have a capacitive gap at their top which provides capacitive loading. The ends of the hairpin resonator were gathered to preserve the high Q of the HTS circuit, to provide a means to switch the resonator, and to keep the radiation loss low.

The filters were designed from a lowpass prototype using the equations in [1]. These equations are for bandstop filters using series-type resonators connected in shunt across a transmission line at quarter-wavelength intervals. The equations in [1] give the required slope parameters x_k for the resonators for a given lowpass prototype and fractional bandwidth. Then using the equation

$$\Delta_k = \frac{Z_o f_o}{2x_k} \tag{1}$$

the 3-dB stop-band-width, Δ_k, can be obtained for each resonator operated by itself connected to a line of impedance, Z_o. Here, f_o from (1) is the center frequency of the stop band. The design of the resonators in Fig. 1 was accomplished by using SONNET© software's Xgeom and EM [2] to analyze various parts of the resonator, and then the parts were pieced together in Touchstone© [3] to model the entire resonator. The spacing between the resonator and the main line was adjusted to obtain the correct coupling (as evidenced by the single resonator having the correct computed 3-dB bandwidth Δ_k), and the height of the resonator was adjusted to obtain the proper center frequency f_o. Once the designs for the individual

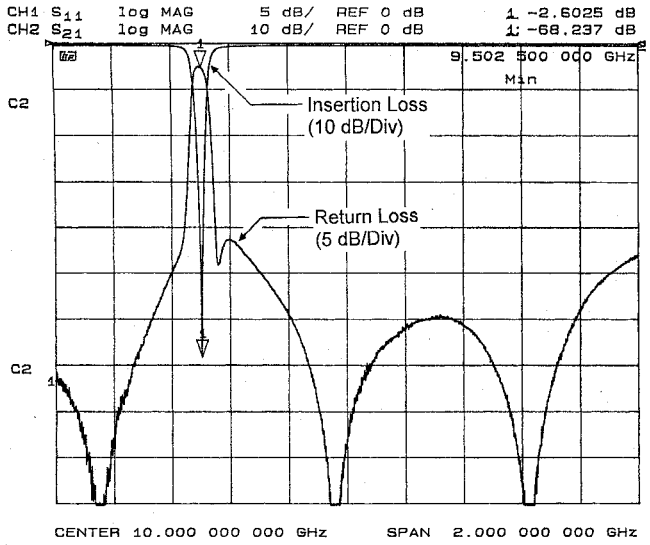

Fig. 2. Three-resonator filter response.

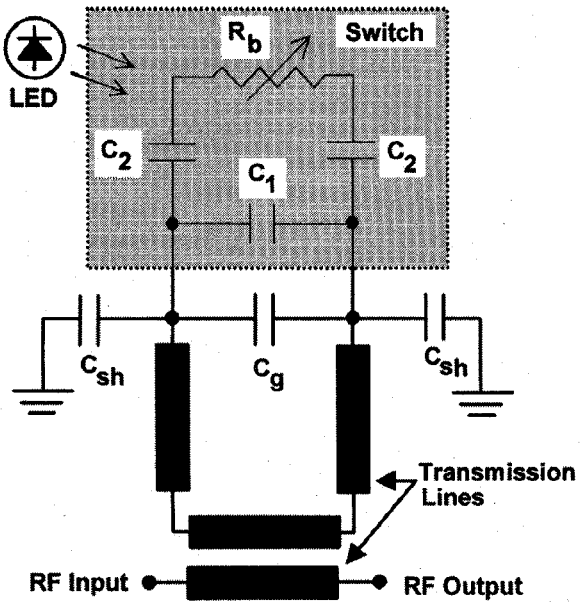

Fig. 3. Equivalent circuit for photosensitive switch integrated with HTS folded hairpin resonator.

resonators of a filter were obtained, they were pieced together to obtain the overall filter design.

B. Fabrication

The filters were fabricated using bi-dielectric shielded stripline [4]. It is like ordinary stripline except that the lower half of the stripline consists of a 20-mil-thick $LaAlO_3$ substrate, while the upper half of the stripline is filled with air. This configuration has the advantage that it provides room for the placement of the photosensitive switches and the use of tuning screws, yet it suppresses radiation and tends to reduce stray coupling between the resonators. Because $LaAlO_3$ has a relative dielectric constant of 24, the electric flux is much larger on the lower ground plane than it is on the upper ground plane. As a result, the current is considerably smaller

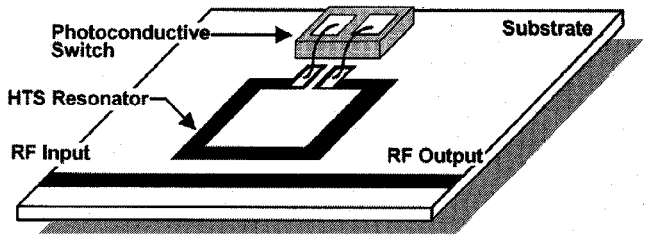

Fig. 4. Layout of photosensitive switch integrated with HTS resonator.

on the non-HTS upper ground plane than it is on the HTS lower ground plane. Because of this and the fact that radiation is suppressed, resonator Q's in the 3000–4000 range were observed without switches. The switches tended to lower the Q to some extent.

Though using bi-dielectric stripline considerably reduced the amount of stray coupling between resonators, because of the relatively large ground plane spacing used (40 mils) it was found to be desirable to use three-quarters of a wavelength spacing between resonators rather then one-quarter wavelength spacing. This does not greatly increase the length of the filter bank as it was found to be feasible to interleave the resonators of the different filters, as the presence of a nearby resonator well off of resonance did not significantly affect the performance of a resonator on resonance. Fig. 2 shows the response of one of the filters. The filters typically have a 3-dB bandwidth of about 70 MHz and a 30-dB bandwidth of about 20 MHz.

III. Photosensitive Switch

A. Switch Model

Circuit analysis of the switch model was performed using two programs: an in house program called Nodal [5], and Touchstone© [3]. The switches were originally modeled as a piece of bulk semiconductor with ohmic contacts. The equivalent circuit model for the resonator and switch is shown in Fig. 3. Computer analysis of the switch model integrated with a resonator showed that the contacts did not need to be alloyed in order for the switch to function as needed with the resonator. This was due to the large capacitance of C_2, approximately 0.5 pF, which is a low impedance at 10 GHz. C_1, whose value is approximately 0.03 pF, is the capacitance between the patterned metal pads of the switch. R_b is the resistance of the bulk semiconductor. In the dark state $R_b > 1$ MΩ and in the illuminated state $R_b < 20\ \omega$. The capacitance of the coupled ends of the resonator, C_g, is approximately 0.08 pF. The shunt capacitance of the resonator, C_{sh}, is approximately 0.08 pF. The capacitance values of the resonator pads were derived from SONNET© software's Xgeom and EM [2] and verified by measurement.

The method of switch attachment entailed gold wire bonding the two-terminal switch to the pads on the coupled ends of the HTS resonator (see Fig. 4).

The model shows that the dark state of R_b must be >10 MΩ in order for the switch to contribute minimal degradation to resonator Q. For a switched loss of approximately 0.03 dB, the

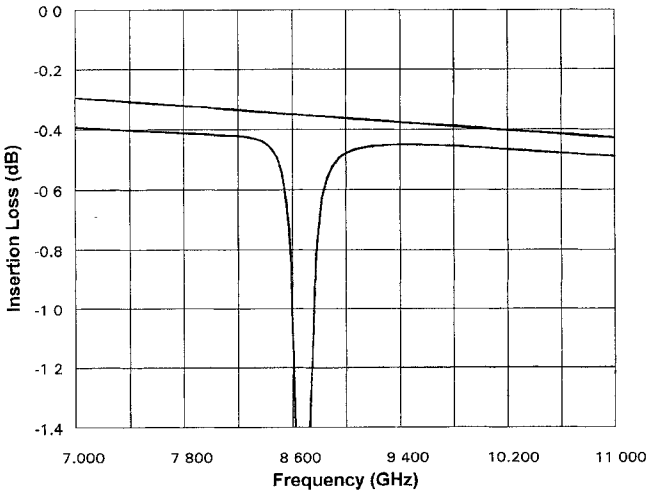

Fig. 5. Nodal simulation of switched filter.

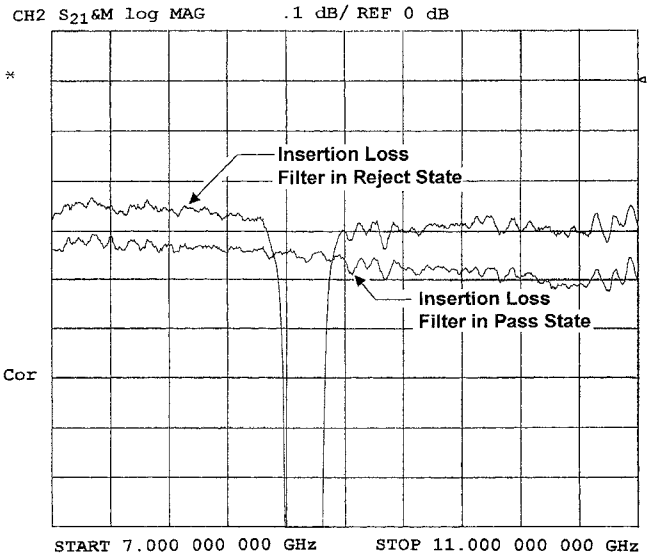

Fig. 6. Switched response of 3-section filter.

illuminated resistance needs to be <20 Ω. The switched loss is defined as the difference between the loss 80 MHz away from the resonant frequency in the reject state and the worst case loss in the pass state in the defined pass band corrected for return loss ripple. Fig. 5 is a simulation from a Nodal model of a three section switched filter. The plot shows the frequency response (S_{21}) of the filter in the reject state and in the illuminated or pass state.

B. Switching Method

Fiber optic cables are used to deliver photons to the photo-switch. Optical switching is more attractive than electrical switching because it avoids the complications associated with having electrical bias and switching-signal connections on each resonator, and also avoids the additional heat conduction that would be associated with the use of electrical conductors. Any extra heat load associated with the device translates into longer cooldown times. There is also no outgassing associated with the glass fiber optic cables. Excessive outgassing can shorten the insulated vacuum time of a dewar.

An LED with an operating wavelength of 880 nm is used to illuminate the switch. The fiber optic cable is positioned intimately with the switch so as to allow for maximum light transfer from the fiber to the switch. The photons bombard the crystal, creating electron hole pairs and thus increase the carrier concentration while decreasing the bulk resistivity.

C. Switch Material Selection

The two materials used to make the photosensitive switches are GaAs and high-resistivity silicon. Both photosensitive materials exhibit a high dark state dc resistance and a low illuminated state dc resistance. When cooled to 77 K, the dark state resistance increases as predicted [6] by the following equation:

$$n_i(T) = 2\left(\frac{2\pi kT}{h^2}\right)^{3/2}(m_n m_p)^{3/4}e^{-Eg/2kT} \qquad (2)$$

due to a decrease in the intrinsic carrier concentration $n_i(T)$. This increase in resistance minimizes resonator Q degradation when the switch is integrated with the HTS resonator. In (2), m_n is the effective mass of an electron and m_p is the effective mass of a hole. Eg is the band gap, h is Planck's constant, k is Boltzmann's constant, and T is temperature.

D. Switch Fabrication

The switches are manufactured from GaAs and n-type silicon wafers. They are fabricated by first patterning a wafer with photo-resist and then sputtering the metal contacts. The GaAs contacts are made from a Ni, Ge, and Au composition. The silicon contacts are made by first depositing Ti-W onto the wafer for good adhesion. Then Au is sputtered to allow for good bond adhesion. The photo-resist is then lifted off and the wafer is thinned to 0.007 in and diced to 0.015 by 0.025 in. The switches are attached to the HTS circuits using polyimide and then gold wire bonded to the coupled ends of the resonator.

E. Measured Switched Results

The circuit was first tested using an HP 8720 Vector Network Analyzer. The packaged filter was bolted to a copper block that is submerged in liquid nitrogen. The measured insertion loss and return loss of a three-section switched filter incorporating GaAs switches is shown in Fig. 6. The switched loss of the filter is approximately 0.1 db in the worst case. This translates into less than 0.04 db per resonator. The silicon switches exhibited a slightly higher switched loss. By increasing the current to the LED that is used to deliver the photons to the silicon switch, the switched loss did improve.

From these results, it is shown that our modeled data correlates very closely with the measured data.

Next, switching times were measured. The switching times of the GaAs switch are approximately 8 μs from the dark state to the illuminated state and approximately 340 μs from the illuminated state to the dark state. The slower switching time (illuminated state to dark state) is due to the deep traps in the GaAs which electrons enter and exit until they finally recombine. This creates a nonexponential decay characteristic

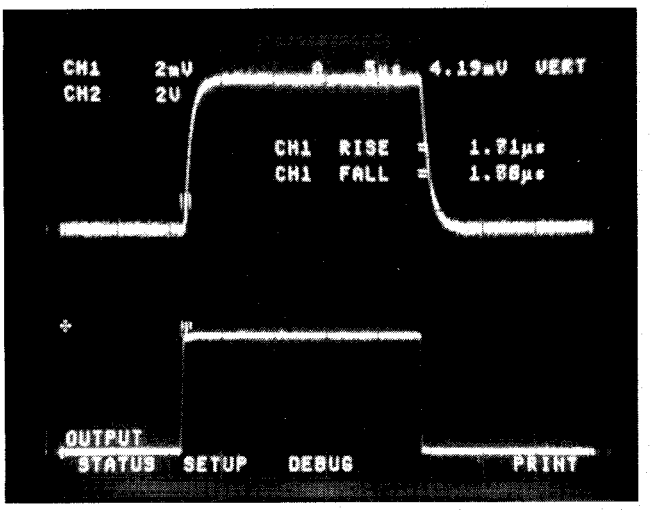

Fig. 7. Switching speed of silicon switch.

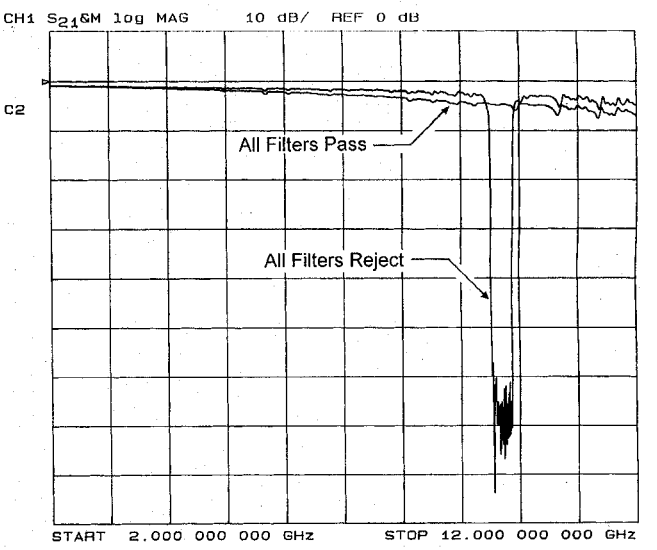

Fig. 8. Wide-band frequency response of a 16-channel switched filter bank.

and slower switching times. The silicon switches exhibited well defined exponential decay with a single time constant. Switching times of less than 5 μs were measured on the silicon devices (see Fig. 7).

Figs. 8 and 9 show the switched response of a 16-channel filter bank [8] which is cooled using liquid nitrogen. Fig. 10 is a photograph of the LN_2 cooled 16-channel switched filter bank assembly. The RF package is mounted on the cold head inside the dewar. The LED's are mounted on the warm side of the dewar wall with the fiber optic cables going from the LED's to the RF package. There is an RF input and RF output on the dewar along with a dc feedthru to supply the switching current to the LED's.

Some work has been done using an FET to switch a microwave circuit [7]. However, the FET biased circuits we tried dequed the folded hairpin resonators due to their low dc impedance.

IV. RF Package

The material selected for the housing needs to allow fast cooldown, be well matched to $LaAlO_3$'s coefficient of thermal expansion, be compatible with the requisite gold plating necessary for wire bonding, and be ridged enough to prevent substrate breakage during assembly and handling.

In the design of the housing and cover, 416 CRES steel is selected based on its machinability, volumetric heat capacity and stiffness. The coefficient of thermal expansion is reasonably well matched to that of $LaAlO_3$. To minimize the heat capacity of the housing and cover, the wall thickness is kept to a minimum at all points possible. The wall thickness is 0.020–0.025 in thick at most places. Attachment of the substrate to the housing is done using heat treated Be-Cu clips. This allows for some release of stresses between the substrate and housing during cooldown, and also allows for easier, safer removal of substrates without breakage. To align the resonators of each filter in frequency, threaded metallic tuners are used in the cover of the housing. These tuners thread into holes in the cover and are centered over each of the resonators in the housing. The tuners provide a tuning rang of ≈200 MHz.

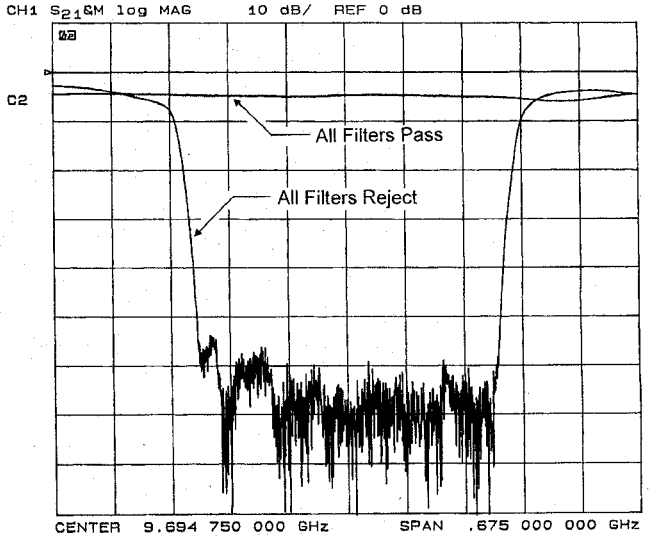

Fig. 9. Narrow-band frequency response of a 16-channel switched filter bank.

The housing also incorporates optical delivery to the photosensitive switches via optical fibers. The fibers enter through holes in the side of the housing which are aligned with the surface of the substrate. Because of the small size of the fiber (0.010 in diam), the holes in the side of the housing are machined to a larger size, into which steel bushings are press fit. The bushings maintain a tight control of concentricity of 0.012 in I.D. with 0.0325 in O.D. and hold the optical fibers in place.

The cover contacts the housing at a "grounding ridge" 0.003-in-wide around the perimeter of the cavity of the housing. This feature is used both to insure electrical continuity around the perimeter and to allow the cooling of the cover to lag behind that of the housing to help insure the most rapid cooling possible.

All threaded hardware used in securing the cover and Be-Cu clips is miniature; 1.10 and 1.00 UNM screws. The cover

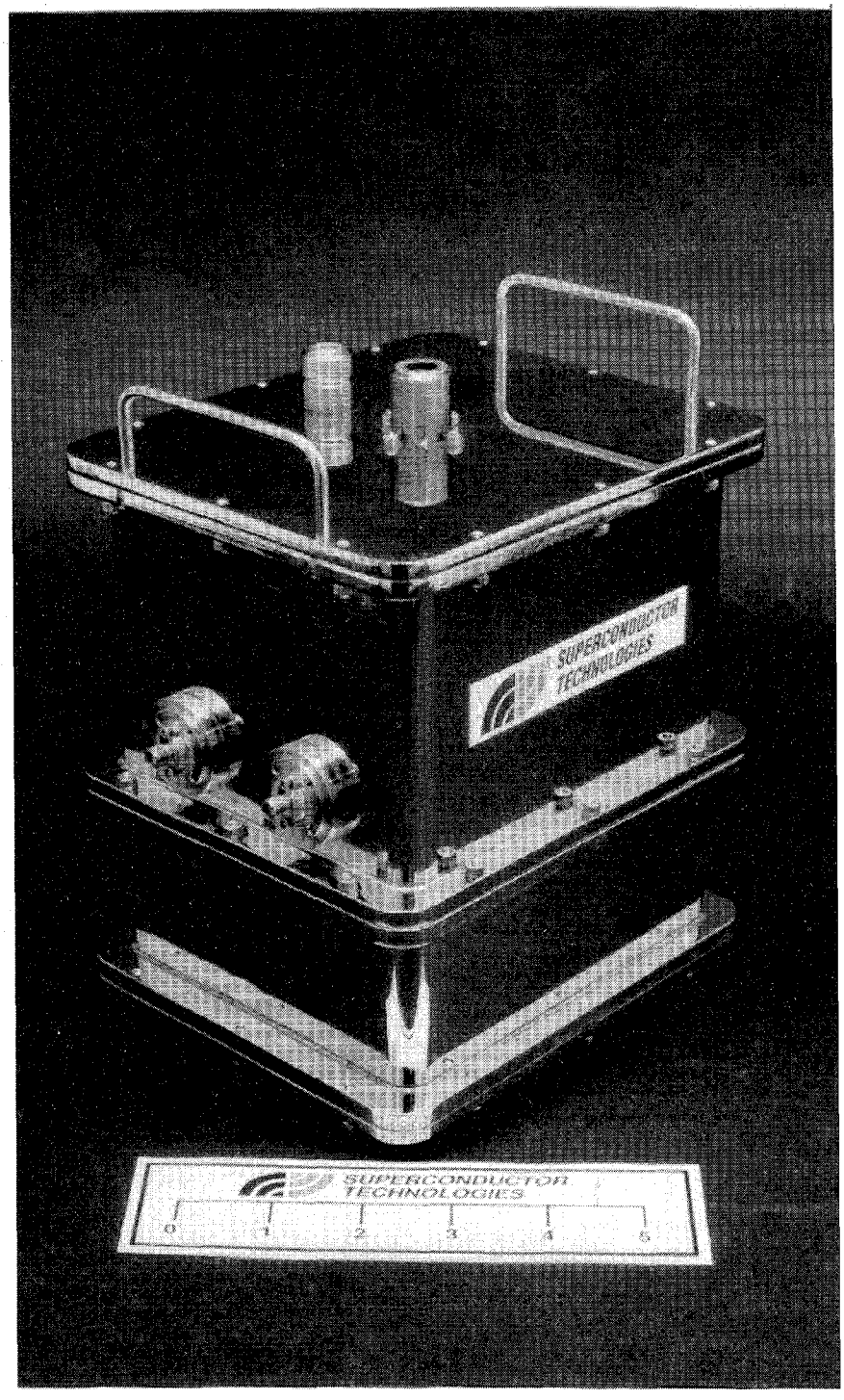

Fig. 10. Photograph of LN_2 cooled 16-channel switched filter bank assembly.

is secured with approximately 60 screws because of its large size ($\approx 0.8 \times 3.8$ in).

The total weight for the housing containing 24 three-section filters, a cover, 72 0–80 thread brass tuners, and all screw hardware is 38 g (1.34 oz).

V. Dewar

The requirements for the dewar are that it be designed for fast cooldown, minimum temperature gradient across the coldstage interfaces, minimum stresses at the cold stage and for minimum heat load to the coldstage. The dewar is designed for either a temporary vacuum seal, using an O-ring and a dessicant, or a permanent vacuum seal, using a welded lid with refireable getters.

The coldstage is an endcap platform made from Aluminum Nitride, selected for its low thermal capacity and high thermal conductivity properties to aid in minimizing the cooldown time. The endcap platform supports the HTS housing, which is mechanically and thermally attached to the endcap. A dessicant

is also temporarily attached to the endcap and can be removed if a permanent vacuum seal is desired. Preliminary analysis shows that the cooldown time will be within the required time of 30 min.

The endcap is brazed to a thin walled Inconel tubing, selected for its low value in thermal conductivity to minimize heat load to the cold stage. The heat load (includes radiation, conduction and device power dissipation) was calculated to be approximately 2.8 W. Calculations also show that the thin walled tubing is rigid enough to withstand a worst case load of 50 g with a natural frequency of 3800 Hz and a deflection of 0.000 03 in.

The tubing is brazed to the outer vacuum housing assembly which consists of a cylindrical flange, utilized to secure the dewar to the cooler flange, and a rectangular vacuum housing. The dc connector and RF feedthrus are welded onto the sides of the rectangular housing wall. LED supports are brazed onto the inside wall of the rectangular housing. The rectangular housing includes a sealing flange. The flange features an o-ring groove for a temporary vacuum seal and a precision machined ledge for welding a permanent vacuum seal.

The temporary cover includes a vacuum valve and is attached to the housing flange with #6-32 screws. The permanent cover includes a tip-off tube assembly, two refireable getters and four getter feedthru leads. The refireable getters along with the feedthru leads are contained within a pill box-like enclosure and covered with a radiation shield made from stainless steel foil.

VI. Cryocooler

The device used to provide and maintain the operating temperature for the HTS bank is a free-piston Stirling cycle cryocooler. A free-piston Stirling cycle cryocooler offers the best solution for this application. It is efficient, compact, quiet and provides high specific cooling per unit weight. In its ideal form, the Stirling cycle has the highest possible efficiency for any thermodynamic cycle. Recent developments suggest that very long life and high reliability can be expected from these machines. These characteristics are very important when considering active cooling for electronic components.

This cooling cycle differs from the vapor compression cycle which is probably the most common means and most familiar method of providing cooling for domestic refrigeration and air conditioning. The cryocooler consists essentially of two moving parts; a piston and a displacer, and uses gaseous helium at about 15 atmospheres of pressure as the working fluid. The piston is electromagnetically driven by a linear motor and the displacer is driven by gas pressure differences in the unit. The system is essentially a tuned mechanical oscillator with the piston and displacer tuned to obtain a phase angle which provides optimum thermodynamic efficiency. The working fluid remains in the gaseous state throughout the cycle and rather than being circulated through a loop, it is oscillated between a heat acceptor stage (where the HTS filter bank is located) and a heat rejector stage at about 60 Hz. High efficiency heat exchangers are located between these two stages.

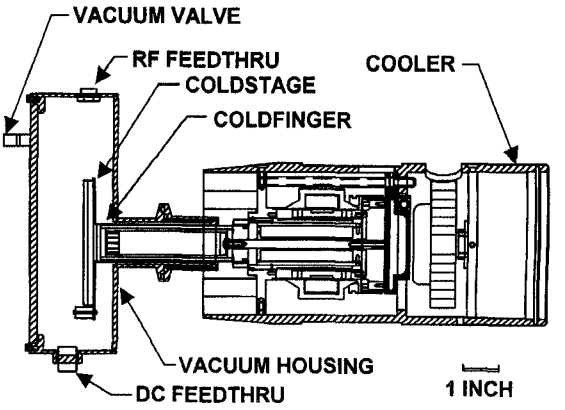

Fig. 11. Cross section of Dewar/Cooler assembly.

Historically, Stirling machines were all kinematically driven. That is, they employ crank shafts and connecting rods used in most positive displacement machinery. The kinematic approach led to a number of problems which limited long life and high reliability. Machines utilizing either gas or flexural bearings use a split configuration and require two linear motors and position sensors for phasing. These machines are generally more complicated and expensive.

In STI's approach, one linear motor is used and phasing is controlled by tuning the system. The moving parts are supported by aerostatic bearings. There are no kinematic mechanisms nor continuously rubbing surfaces in the machine. Some of the compressed helium is supplied to gas bearings pads in the moving parts for lubrication. Frictional wear is therefore eliminated. Another key feature which improves life and reliability is the use of a moving magnet linear motor with a coil, external to the pressurized gas volume. This arrangement minimizes the contamination of the pressurized Helium, eliminates the necessity for an electrical feedthru through the pressure wall and allows easy cooling for the motor coils. Gaseous contamination could be a major problem in the operation of cryocoolers because it freezes in the cold end and affects the efficiency of the heat exchangers thereby affecting the performance of the cryocooler. Helium containment is another serious concern for high reliability. The pressurized vessel of the machine is an all metal container which has been vacuum brazed and electron beam welded. Excellent helium hermetically is achieved and forced air convection is used to cool the unit. A cross section of the Dewar/Cooler assembly is shown in Fig. 11. Fig. 12 shows a STI cryocooler integrated with a vacuum dewar.

VII. Applications

Applications for the new planar HTS RF circuit technology are in every communications system. The HTS band-reject switched filters present a new solution to RF problems that are becoming increasingly more troublesome as the airwaves become saturated with signals. These signals are becoming more sophisticated, with frequency agility becoming quite common. This presents a challenging electromagnetic environment that a receiver has to cope with. For an Electronic Warfare (EW)

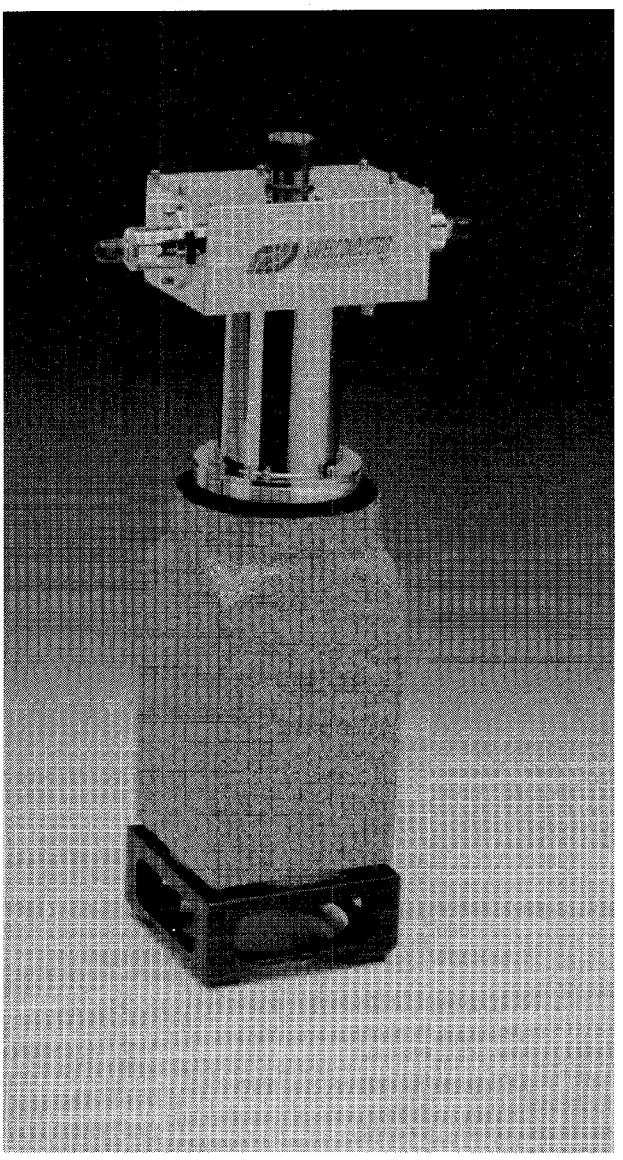

Fig. 12. Stirling cycle cryocooler integrated with a vacuum dewar.

receiver all signals have to be identified and categorized, including friendly ones, so that lethal signals are intercepted and appropriate action taken. Missed or misidentified signals can have catastrophic consequences in a combat scenario. The use of switchable band-reject HTS filters to excise harmful interfering signals on a time varying basis can greatly enhance both EW and communication system performance. Tests conducted by the US Air Force on a reconfigurable front-end filtering system, of the type described in this paper, have demonstrated significant improvements to the performance of EW receivers at X-band frequencies.

Application of these techniques is not limited to EW receivers. Both military and commercial communication networks suffer from capacity limiting interference. This in general is due to unintentional interference, but the resulting lost communication channel has important consequences and can result in lost revenue for the latter application. Extension of this technology to other frequencies (both higher and lower) can produce the same benefits as already demonstrated. By using both band-pass and band-reject filters in conjunction, exceptional flexibility in the pass band and stop band characteristics could be achieved. Incorporating switching into the filter banks would allow for an adaptive characteristic that could be altered to account for varying interference problems. Such a complexity of filtering functions is not practical using traditional technology.

VIII. Conclusion

The work presented in this paper forms the basis for continued development in the area of switchable HTS filter banks. We have demonstrated a fast silicon photosensitive switch which can be integrated with HTS resonators to form filters. The three-section HTS band-reject filters are optically switched with low insertion loss using GaAs photosensitive switches and are cascaded to form filter banks. Digital control of the band-reject filters allows the user to arbitrarily define any reject or pass band within the filter bank. The filterbank is housed in a vacuum dewar and cooled with a Stirling cycle cryocooler.

Acknowledgment

The authors would like to thank the film manufacture and fabrication teams at Superconductor Technologies Inc.

References

[1] G. L. Matthaei, L. Young, and E. M. T. Jones, *Microwave Filters, Impedance-Matching Networks, and Coupling Structures.* Dedham, MA: Artech, 1980, pp. 725–773.
[2] Electromagnetic analysis software by SONNET Software, Inc., Liverpool, NY, 13090.
[3] Linear circuit simulation software produced by HP-EEsof, Westlake Village, CA.
[4] R. K. Hoffman, *Handbook of Microwave Integrated Circuits.* Norwood, MA: Artech, 1983, pp. 349–350.
[5] A linear circuit simulation software package developed by R. Forse at Superconductor Technologies, Inc., Santa Barbara, CA, 93111.
[6] B. G. Streetman, *Solid State Electronic Devices,* 2d ed. Englewood Cliffs, NJ: Prentice-Hall, 1980, pp. 75–77.
[7] J. L. Freeman, S. Ray, D. L. West, and A. G. Thompson, "Optoelectronic devices for unbiased microwave switching," in *IEEE MTT-S Dig.,* pp. 673–676.
[8] K. Raihn, N. Fenzi, E. Soares, and G. Matthaei, "An optical switch for high temperature superconducting microwave band reject resonators," in *IEEE MTT-S Dig.,* pp. 187–190.

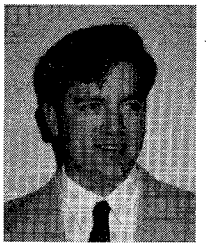

Kurt F. Raihn was born in Portola, CA, in 1962. He received the B.S. degree in electrical engineering from San Diego State University (SDSU) in 1986. While attending SDSU, he was an engineering intern from 1982 to 1986 at the Naval Oceans System Center Microwave/Millimeter-wave Research and Development Branch, Point Loma, CA.

He was with Spacek Labs Inc., Santa Barbara, CA, from 1986 to 1993, where he designed and tested microwave and millimeter-wave components and sub-systems. He is currently with Superconductor Technologies Inc., Santa Barbara, where he provides engineering support for product, contract and IR&D efforts. He has authored several papers and holds two patents.

Neal O. Fenzi (M'93) received the B.S.E.E. degree from New Mexico State University, Las Cruces, in 1982.

From 1982 to 1984, he was with the Microwave Filters Division of Hughes Aircraft Co., Space and Communications Group, designing and building filters for satellite communications. From 1984 to 1991, he was with Amplica, Inc., designing microwave amplifiers and subassemblies for the telecommunications and military markets. Since 1991, he has been an Engineering Section Head with Superconductor Technologies Inc., Santa Barbara, CA. He has authored many papers, holds one patent in the HTS field, and his area of interest is applying HTS technology to the design of useful products.

Gregory L. Hey-Shipton (M'81) received the Ph.D. degree from Leeds University, U.K., in 1978.

He was with the Watkins-Johnson Company from 1978 to 1991 at several locations, finally as Department Manager of the Subsystems Product Engineering Department, Palo Alto, CA. He joined Superconductor Technologies Inc., Santa Barbara, CA, in June 1991, as the Engineering Manager and was made Vice President in March 1992. He is currently the Manager of the Government Business Unit at STI and is involved in the development of new RF and microwave thin film HTS circuits, and develops products for sale to government customers.

Elna R. Saito received the B.S. and M.S. degrees in mechanical engineering from University of California, Santa Barbara, in 1982 and 1988, respectively.

From 1982 to 1994, she was employed at Santa Barbara Research Center, a subsidiary of GM-Hughes, were she worked as a design engineer on high vacuum cryogenic assemblies for infra-red sensors in military and space applications. Currently, she is a Cryogenics Engineer at Superconductor Technologies Inc., Santa Barbara, where she works with both the commercial and government business units designing cryogenic dewars for HTS applications. She is an author of several papers.

P. Vince Loung received the B.E., M.E. (Mech.) degrees from McGill University, Montreal, Québec, Canada, and the M.S. degree from West Coast University, Los Angeles, CA.

He is presently a program manager at Superconductor Technologies Inc., Santa Barbara, responsible for cryocooling. He is the principal investigator on ARPA and NASA funded programs on Stirling and Pulse Tube cryocooler design and development. Prior to STI, he was Mechanical Engineering Manager at Amber Raytheon and a Project Design Engineer at Santa Barbara Research Center, a subsidiary of Hughes Aircraft, designing, developing and manufacturing infra-red imaging and tracking cameras and sensors for space, aerospace and commercial applications. He has been engaged in cryogenics and high vacuum systems R&D and design for semiconductor processing equipment at Varian and MMR Technologies.

David L. Aidnik received the B.S. degree in physics from the University of California, Santa Barbara, in 1989.

From 1985 to 1989, he was with Honeywell and Watkins Johnson at the Spacekom Microwave Center, Santa Barbara, where he worked in the design and manufacture of broadband mm-wave mixers, frequency multipliers and subsystems. From 1989 to 1991, he was with Amplica, Newbury Park, CA, where he was a design engineer working in the development of a GPS receiver front end for military application. Since joining STI in 1991 as a design engineer, he has been involved in the development of several microwave systems in the Government Products Group. He has co-authored several technical papers on applied superconductivity in the microwave field.